THIC STRUCTURES FOR RF BEAMFORMING

Yuan-Pei Lin and Shang-Ho (Lawrence) Tsai

Dept. Electrical Engr., National Chiao Tung Univ., Hsinchu, Taiwan

ABSTRACT

Recently it is shown that the maximum MIMO beamforming gain can be achieved using only one RF (radio frequency) chain. This is done by implementing the beamformer using Two analog pHase shIfters for each Coefficient (THIC). In this paper we analyze the quantization error of the beamforming coefficients (weights) when the phase shifters used in THIC are of finite resolution. An alternative THIC structure is proposed. The new structure, having the same beamforming gain when the phases can take on continuum values, behaves differently upon quantization. It can achieve a smaller quantization error through proper allocation of quantization bits between the two phase shifters. Simulations are given to demonstrate that a performance very close to the full MIMO beamforming gain can be achieved using phase shifters of low resolution.

1. INTRODUCTION

Beamforming with multiple transmit and receive antennas are known to achieve a beamforming gain that improves with the number of antennas. Recent advances show that it is feasible to use a large number of antennas, particularly in millimeter wave (mmWave) communication systems where the wavelength is small [1]. However cost and power constraint often prohibit having one dedicated RF chain for each antenna. An innovative technique called hybrid beamforming have been proposed to overcome the RF limitation. With hybrid beamforming [2][3], analog processing of RF signals is combined with digital processing in the baseband to improve the performance within the RF chain constraint. Analog processing, due to power and complexity consideration, is typically implemented using phase shifters [3]. It is shown in [2] that having two RF chains is sufficient to achieve the full beamforming gain. To exploit the sparsity nature of mmWave channels, the analog precoder proposed in [3] consists of antenna response vectors appropriately chosen using orthogonal matching pursuit. The digital precoder can further enhance the system performance when there is more than one RF chain. Recently, based on the work of [2], it is further shown that [4] the number of RF chain for a beamforming system can be reduced to only one when the implementation of the beamformer uses Two pHase shIfters for each Coefficient (THIC). In practical implementation, the quantization of the phases cause a degradation to the beamforming gain [5][6]. As precise phase control is costly, it is desirable to use phase shifters of low resolution.

In this paper we consider two implementation structures for an analog beamformer using THIC. The first one is taken directly from [4] and the second one is derived from the first. The two structures achieve the full beamforming gain when the phase shifters are not quantized, but they behave differently in the presence of quantization. We analyze the mean square quantization error for the two structures and show that the errors can be given in terms of the average quantization bits. With the second structure, the quantization errors of the two phase shifters do not contribute to the overall quantization error in the same manner. With appropriate allocation of the quantization bits, it achieves a smaller error and a performance close to full MIMO beamforming gain using phase shifters of low resolution. With THIC, each coefficient is implemented using two phase shifters, which seemingly increases the number of phase shifters. However simulations show that, due to better approximation of the optimal beamformer, it actually reduces the number of RF chains for a given total number of phase shifters.

2. SYSTEM MODEL

Consider a wireless system with N_t transmit antennas and N_r receive antennas. The channel is modeled by an $N_r \times N_t$ memoryless matrix $\mathbf{H}$ with $N_r \times 1$ channel noise $\mathbf{n}$. We assume the channel is slow fading so that the channel does not change during each channel use. The noise vector $\mathbf{n}$ is assumed to be additive white Gaussian with zero mean and variance σ_n^2. Suppose there is only RF chain at the transmitter and the receiver. The input of the transmitter beamformer $\mathbf{f}$ is s. The transmitter output is $\rho\mathbf{f}s$, where ρ is a normalization constant such that the transmisson power is P_t. The receiver is a $1 \times N_r$ vector $\mathbf{g}$ and the receiver output is $\hat{s} = \rho\mathbf{gHfs} + \mathbf{gn}$.

This work was supported in parts by National Science Council, Taiwan, R. O. C., under NSC 98-2221-E-048-MY3 and International Research Center of Excellence on Advanced Bioengineering Grant NSC 99-2911-I-009-101.

978-1-5090-3009-5/17/$31.00 ©2017 IEEE

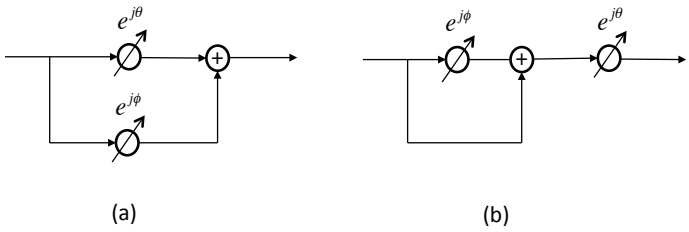

Figure 1: Phase shifter implementation of a beamforming weight, (a) Structure I, and (b) Structure II.

3. QUANTIZATION OF PHASE SHIFTERS

It is shown in [4] that any complex number $c = re^{j\alpha}$ with modulus $r \leq 2$ can be expressed as $c = e^{j\theta} + e^{j\phi}$, where

$$\theta = \alpha - \cos^{-1}(r/2), \quad \phi = \alpha + \cos^{-1}(r/2).$$

This result suggests that the scaling of a number x by a coefficient c can be implemented as in Fig. 1(a). When the phases θ and ϕ are quantized to a finite set of values, so is c. Alternatively, we can express c as

$$c = e^{j\theta}(1 + e^{j\phi}), \tag{1}$$

where θ and ϕ are now related to the magnitude and phase of c in a different manner. The expression in (1) gives rise to the implementation structure in Fig. 1(b), which also uses two phase shifters and a combiner. The two structures in Fig. 1 yield the same result when θ and ϕ are not quantized. In the presence of quantization they behave differently. In the following we consider the quantization of a complex coefficient $c = re^{j\alpha}$ with $r \leq 2$ for the above two structures by quantizing the phases θ and ϕ in Fig. 1. For the convenience of quantization error analysis, the following assumptions are made in the quantization of θ and ϕ.

A1. The quantization errors of θ and ϕ are uncorrelated. That is $\delta_\theta = \hat{\theta} - \theta$ and $\delta_\phi = \hat{\phi} - \phi$ are uncorrelated.

A2. When a phase θ is quantized to $\hat{\theta}$, the quantization error δ_θ is assumed to be uncorrelated with θ, and uniformly distributed over the interval $[-\Delta_\theta/2, \Delta_\theta/2)$, where Δ_θ is the quantization step size.

These two assumptions, commonly used in the analysis of quantization error [7], is generally valid for high rate quantization, eg., the number of quantization bits $b \geq 4$. Let θ be drawn from an interval of length V and the number of bits for quantizing θ be b_θ, then $\Delta_\theta = V2^{-b}$. In this case the variance of quantization error $\sigma^2_{\delta_\theta}$ is given by

$$\sigma^2_{\delta_\theta} = \frac{1}{12}\Delta^2_\theta = \frac{V^2}{12}2^{-2b_\theta}. \tag{2}$$

Although high quantizer resolution is assumed in the derivations, we will see in the simulation examples that the result is accurate even in low resolution case.

3.1. Quantization: Structure I

In Structure I, a weight $c = re^{j\alpha}$ is implemented as $e^{j\theta} + e^{j\phi}$. When θ and ϕ are quantized to $\hat{\theta}$ and $\hat{\phi}$, the corresponding quantized weight is $\hat{c} = e^{j\hat{\theta}} + e^{j\hat{\phi}}$. The quantization error $E[|\hat{c} - c|^2]$ can be approximated in terms of the quantization errors of θ and ϕ as to be given in the following Lemma.

Lemma 1 *Consider a random variable $c = e^{j\theta} + e^{j\phi}$ that is quantized by quantizing θ and ϕ. With high resolution quantization, the effective mean square error $MSE_1 = E[|\hat{c} - c|^2]$ for Structure I can be approximated as*

$$MSE_1 \approx \sigma^2_{\delta_\theta} + \sigma^2_{\delta_\phi}, \tag{3}$$

where $\sigma^2_{\delta_\theta}$ and $\sigma^2_{\delta_\phi}$ are, respectively, the variances of the quantization errors $\delta_\theta = \hat{\theta} - \theta$ and $\delta_\phi = \delta_\phi - \phi$.

A proof of Lemma 1 can be found in Appendix A. For $0 \leq r \leq 2$ and $0 \leq \alpha < 2\pi$, the ranges of θ and ϕ are both from 0 to 2π. Thus the quantization step sizes for quantizing θ and ϕ are $\Delta_\theta = 2\pi 2^{-b_\theta}$ and $\Delta_\phi = 2\pi 2^{-b_\phi}$, where b_θ and b_ϕ are, respectively, the number of bits used for quantizing θ and ϕ. Using the variance formula in (2), we obtain the effective quantization error $MSE_1 = \frac{\pi^2}{3}(2^{-2b_\theta} + 2^{-2b_\phi})$. In this case, we see the quantization errors δ_θ and δ_ϕ contribute equally to the overall MSE. For a given average number of quantization bits b, we can choose $b_\theta = b_\phi = b$.

3.2. Quantization: Structure II

Any scalar $c = re^{j\alpha}$ with modulus $r \leq 2$ can also be written as $c = e^{j\theta}(1 + e^{j\phi})$, where

$$\theta = \alpha - \cos^{-1}(r/2), \quad \phi = 2\cos^{-1}(r/2). \tag{4}$$

This leads to the implementation in Structure II (Fig. 1(b)). When θ and ϕ are quantized to $\hat{\theta}$ and $\hat{\phi}$, the corresponding quantized weight is $\hat{c} = e^{j\hat{\theta}}(1 + e^{j\hat{\phi}})$. Like Structure I, the quantization error $E[|\hat{c} - c|^2]$ can be approximated in terms of the quantization errors of θ and ϕ.

Lemma 2 *Consider the quantization of a random variable $c = e^{j\theta}(1 + e^{j\phi})$. When θ and ϕ are quantized to $\hat{\theta}$ and $\hat{\phi}$, effectively c is quantized to $\hat{c} = e^{j\hat{\theta}}(1 + e^{j\hat{\phi}})$. With high resolution quantization, the effective quantization error $MSE_2 = E[|\hat{c} - c|^2]$ for Structure II can be approximated as*

$$MSE_2 \approx E[r^2]\sigma^2_{\delta_\theta} + \sigma^2_{\delta_\phi}, \tag{5}$$

where $\sigma^2_{\delta_\theta}$ and $\sigma^2_{\delta_\phi}$ are, respectively, the variances of the quantization errors $\delta_\theta = \hat{\theta} - \theta$ and $\delta_\phi = \hat{\phi} - \phi$.

A proof is give in Appendix B. For $0 \le r \le 2$ and $0 \le \alpha < 2\pi$, the range of θ is from 0 to 2π. Unlike Structure I, the range of ϕ now is from 0 to only π. This is because $\phi = 2\cos^{-1}(r/2)$ and r is nonnegative. Thus the step sizes for quantizing θ and ϕ are, respectively, $\Delta_\theta = 2\pi 2^{-b_\theta}$ and $\Delta_\phi = \pi 2^{-b_\phi}$, where b_θ and b_ϕ are, respectively, the number of bits used for quantizing θ and ϕ. Therefore the variances of δ_θ and δ_ϕ are respectively,

$$\sigma^2_{\delta_\theta} = \frac{\pi^2}{3}2^{-2b_\theta}, \sigma^2_{\delta_\phi} = \frac{1}{4}\frac{\pi^2}{3}2^{-2b_\phi}, \tag{6}$$

We obtain the effective quantization error

$$MSE_2 \approx \frac{\pi^2}{3}\left(E[r^2]2^{-2b_\theta} + \frac{1}{4}2^{-2b_\phi}\right). \tag{7}$$

We see the quantization errors δ_θ and δ_ϕ do not contribute to the overall MSE in the same way. Suppose the average number of bits that can be used for quantizing θ and ϕ is b and we are allowed to allocate bits between θ and ϕ. Let b_θ and b_ϕ be the numbers of bits that are used for quantizing θ and ϕ, respectively. Then the bit allocation problem becomes

$$\min_{b_\theta, b_\phi} MSE_2, \quad \text{subject to } (b_\theta + b_\phi)/2 = b.$$

The bit allocation problem can be solved by applying arithmetic mean–geometric mean inequality on the expression in (7) as in Appendix C of [8]. The optimal solutions of b_θ and b_ϕ are $b_\theta = b + \frac{1}{2}\log_2\left(2\sqrt{E[r^2]}\right)$ and $b_\phi = 2b - b_\theta$.

In the above derivation of MSE_2, the two phases θ and ϕ are quantized separately. One is quantized without consideration of the other. Observe that, instead of (4), we can also determine θ and ϕ using $\phi = 2\cos^{-1}(r/2)$ and $\theta = \alpha - \phi/2$. If we first quantize ϕ to $\hat{\phi}$, the desired unquantized value of θ is now changed to $\alpha - \hat{\phi}/2$, which can then be quantized to obtain $\hat{\theta}$. Such an approach, still employing only scalar quantization, quantizes θ and ϕ jointly and has a smaller quantization error as we see next. Let the quantized θ be $\hat{\theta} = \alpha - \hat{\phi}/2 + \delta_\theta$. Thus $\hat{c} = e^{j(\hat{\theta}+\hat{\phi}/2)}2\cos(\hat{\phi}/2)$ can be expressed as $\hat{c} = e^{j(\alpha+\delta_\theta)}2\cos(\hat{\phi}/2)$. Now the equivalent phase is affected only by the quantization error δ_θ rather than both δ_θ and δ_ϕ as in the previous case. When θ and ϕ are thus quantized, the MSE can be approximated as

$$MSE_2' \approx E[r^2]\sigma^2_{\delta_\theta} + (1 - E[r^2]/4)\sigma^2_{\delta_\phi}, \tag{8}$$

which is smaller than that in (7) by $E[r^2]/4\sigma^2_{\delta_\phi}$. A proof of (8) can be found in Appendix C. The ranges of θ and ϕ are respectively $[0, 2\pi)$ and $[0, \pi]$, the same as before. Using (6), we can rewrite MSE_2' as

$$MSE_2' \approx \frac{\pi^2}{3}\left(E[r^2]2^{-2b_\theta} + \frac{1}{16}(4 - E[r^2])2^{-2b_\phi}\right). \tag{9}$$

Note that in such a joint quantization of θ and ϕ, only scalar quantization is needed. Quantization is done the same way as discussed earlier except for the computation of the desired θ.

As an example, consider the quantization of a random variable $c = re^{j\alpha}$, where r is uniformly distributed over the interval $[0, 2]$ and α is uniformly distributed over $[0, 2\pi)$. Fig. 2 shows the mean square quantization error for Structure I and the two quantization schemes of Structure II by averaging over 10^5 realizations. The theoretical mean square errors are computed using the formulas in (3), (7), and (9) Although the quantization error is analyzed under the assumption of high quantization resolution, we can see from Fig. 2 the results are accurate even for low resolution quantization too, except for the case of very low rate quantization $b = 1$ for Structure I. We observe that Structure II with joint scalar quantization has a smaller error than that with separate quantization and the error is around half that of Structure I. For the beamforming simulation in Sec. 5, joint scalar quantization will be used for Structure II.

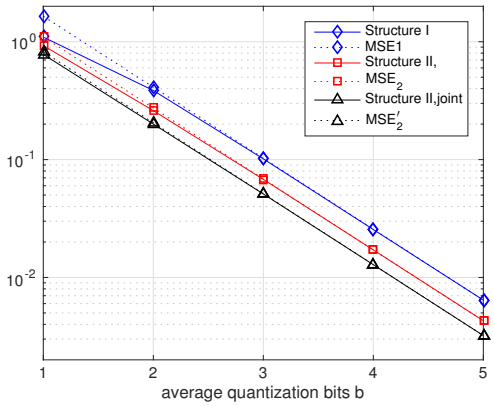

Figure 2: Mean square quantization error as a function of the average quantization bits b.

4. QUANTIZATION OF BEAMFORMERS

Let us first consider the case when there is no quantization. When there is no quantization, the optimal beamformer is related to the singular vectors of the channel $\mathbf{H}$. Let $\mathbf{v}$ and $\mathbf{u}$ be respectively the right and left singular vectors corresponding to the largest singular value λ of the channel. Then the optimal beamforming vector is $\mathbf{v}$ and the optimal receive combining vector is $\mathbf{u}^\dagger$, where $\mathbf{u}^\dagger$ denotes the transpose and conjugate of $\mathbf{u}$. The optimal unconstrained signal to noise ratio is $SNR_{opt} = \lambda_0^2 P_t/\sigma_n^2$.

When the phase shifters are of finite resolution, the transmit beamformer and receive combiner are only quantized

versions of the optimal beamformer and combiner. Given the quantized beamformer $\hat{\mathbf{f}}$, the optimal unconstrained combining vector is no longer the left singular vector of $\mathbf{H}$ corresponding to the largest singular value. It is the one that is matched to $\mathbf{H}\hat{\mathbf{f}}$. In what follows, we summarize the steps for quantizing the beamformer and combiner. (1) For a given channel $\mathbf{H}$, we compute $\mathbf{v}$, the right singular vector that corresponds to the largest singular value of $\mathbf{H}$. (2) Apply a normalization factor β_f so that the entries of $\mathbf{f} = \beta_f \mathbf{v}$ have modulus ≤ 2. (3) Quantize each entry of $\mathbf{f}$ using one of the structures discussed in Sec. 3. (4) Compute the desired combiner $(\mathbf{H}\hat{\mathbf{f}})^\dagger$ and normalize it to obtain $\mathbf{g} = \beta_g(\mathbf{H}\hat{\mathbf{f}})^\dagger$, where β_g is such that the entries of $\mathbf{g}$ have modulus ≤ 2. (5) Quantize $\mathbf{g}$ to $\hat{\mathbf{g}}$ as in Step (3).

In the above discussion, THIC with finite-resolution phase shifters is considered for beamforming. We can also apply THIC when multiple substreams are transmitted and precoders used, as detailed in [11].

5. SIMULATIONS

For the evaluation of the proposed quantization schemes, we adopt the clustered channel representation [3][10]. The channel consists of N_{cl} clusters and each cluster contains N_{ray} propagation paths,

$$\mathbf{H} = \frac{1}{\sqrt{N_{cl}N_{ray}}} \sum_{k=1}^{N_{cl}} \sum_{\ell=1}^{N_{ray}} \alpha_{k\ell} \mathbf{a}_r(\phi_{kl}^r)\mathbf{a}_t^\dagger(\phi_{kl}^t), \qquad (10)$$

where $\alpha_{k\ell}$ is the complex gain of the ℓth ray in the kth cluster, assumed to be zero mean Gaussian and of unity variance. The vectors $\mathbf{a}_t(\phi_{kl}^t)$ and $\mathbf{a}_r(\phi_{kl}^r)$ are, respectively, the transmit and receive antenna array response vectors, determined respectively by angle of departure ϕ_{kl}^t and angle of arrival ϕ_{kl}^r. The angles ϕ_{kl}^t and ϕ_{kl}^r are of a truncated Laplacian distribution [9][10], with means $\bar{\phi}_k^t$ and $\bar{\phi}_k^r$, and standard deviations $\sigma_{\phi_k}^t$ and $\sigma_{\phi_k}^r$, respectively. The means $\bar{\phi}_k^t$ and $\bar{\phi}_k^r$ are assumed to be uniformly distributed over $[0, 2\pi)$. The array response for a uniform linear array with N antennas is given by $\mathbf{a}(\phi) = \left[1 \quad e^{j2\pi d \sin(\phi)} \cdots e^{j2\pi d(N-1)\sin(\phi)}\right]^T$ where d is the antenna spacing normalized by the wavelength.

Consider a beamforming system with one RF chain over a channel described by (10) with $d = 1/2$ and $N_t = N_r = 16$. The standard deviations $\sigma_{\phi_k}^t$ and $\sigma_{\phi_k}^r$ are 7.5°, $N_{cl} = 3$, $N_{ray} = 10$ and 10^5 channels are used in the performance evaluation. Fig. 3(a) shows the bit error rate (BER) performance when QPSK symbols are transmitted. The coefficients of the optimal beamforming and combining vectors are quantized using Structures I or II in Fig. 1 with $b = 1.5$, and 2 bits, where b is the average number of quantization bits. Compared to the unconstrained optimal beamforming,

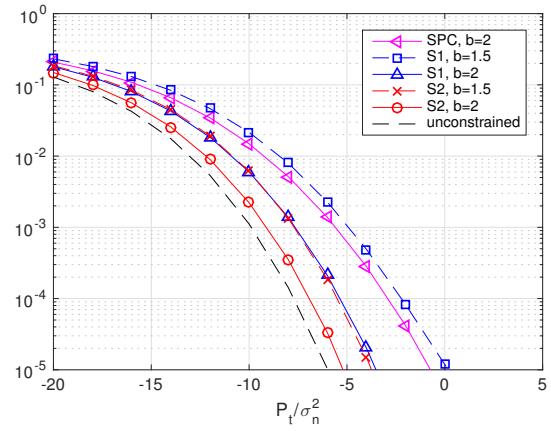

(a)

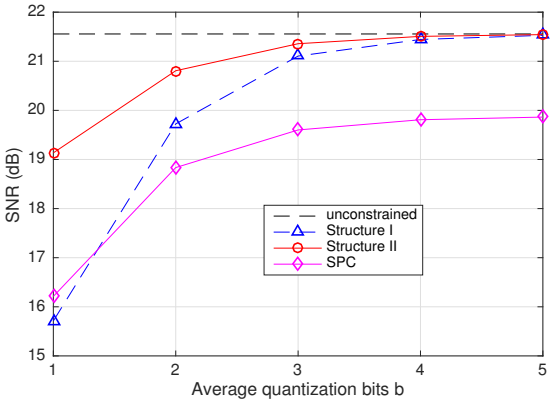

(b)

Figure 3: Beamforming system with $N_t = N_r = 16$, (a) BER performance, and (b) average SNR vs. average number of quantization bits.

the SNR degradation for $b = 2$ is around 0.8 dB for Structure II and 2.5 dB for Structure I when the BER is 10^{-5}. For $b = 1.5$, the angles θ and ϕ in both structures are quantized using 2 bits and one bit, respectively. The performance of Structure II with $b = 1.5$ is about the same as that of Structure I with $b = 2$ bits; a simpler one-bit quantizer can be used for quantizing ϕ in Structure II. Also shown in Fig. 3(a) are the curves of sparse precoding and combining (SPC) [3] with two RF chains at the transmitter and receiver. With two RF chains, the SPC analog precoder consists of two constant-modulus beamsteering vectors, each corresponding to an appropriately chosen propagation path. In this case the number of phase shifters used in SPC is the same as that in Structure I or II, which requires two phase shifters for each antenna weight. With either Structure I or II, the beamformer is a quantized version of the optimal beamformer; the direction of the beam better matches that of the optimal beamformer and a performance closer to that of the optimal beamformer can be achieved. In Fig. 3(b), the average

overall SNR of the quantized beamformer is compared with the optimal unconstrained SNR. While the performances of both structures get very close to that of the optimal case as b increases, a significant difference can be observed in low rate quantization.

6. CONCLUSION

In this paper, we consider the quantization of phase shifters for practical analog beamforming. Based on an earlier result that cleverly expresses a beamforming weight using two phase shifters, we analyze the quantization error of a beamforming weight when phase shifters are quantized. An alternative implementation of beamforming weight, also using two phase shifters, is proposed and shown to achieve a smaller quantization error and a performance close to full MIMO beamforming gain.

Appendix A. Proof of Lemma 1

The quantized $\hat{c} = e^{(j\theta+j\delta_\theta)} + e^{(j\phi+j\delta_\phi)}$ can be written as four terms: $\hat{c} = \cos(\theta+\delta_\theta) + j\sin(\theta+\delta_\theta) + \cos(\phi+\delta_\phi) + j\sin(\phi+\delta_\phi)$. The first term $\cos(\theta+\delta_\theta)$ can be expressed as $\cos(\theta)\cos(\delta_\theta) - \sin(\theta)\sin(\delta_\theta)$. When quantization resolution is high, δ_θ and δ_ϕ are small and thus $\cos(\delta_\theta) \approx 1$ and $\sin(\delta_\theta) \approx \delta_\theta$. So the first term $\cos(\theta+\delta_\theta)$ can be approximated as $\cos\theta - \delta_\theta \sin\theta$. Applying similar approximations on the remains three terms of $\hat{c}$, we obtain $\hat{c} \approx \cos\theta - \delta_\theta\sin\theta + j(\sin\theta + \delta_\theta\cos\theta) + \cos\phi - \delta_\phi\sin\phi + j(\sin\phi + \delta_\phi\cos\phi)$. The quantization error is $\hat{c}-c \approx -\delta_\theta\sin\theta - \delta_\phi\sin\phi + j(\delta_\theta\cos\theta + \delta_\phi\cos\phi)$. Using this approximation and the assumptions that δ_θ and δ_ϕ are uncorrelated and have zero mean, we can approximate the mean square quantization error as $MSE_1 \approx \sigma^2_{\delta_\theta} + \sigma^2_{\delta_\phi}$.

Appendix B. Proof of Lemma 2

The quantization error can be rewritten as $\hat{c} - c = \cos(\theta + \delta_\theta) + j\sin(\theta+\delta_\theta) + \cos(\theta+\phi+\delta_\theta+\delta_\phi) + j\sin(\theta+\phi+\delta_\theta+\delta_\phi) - e^{j\theta} - e^{j(\theta+\phi)}$, which, using angle sum formulas for cosine and sine functions, can be further expressed as $\hat{c}-c = \cos\theta\cos\delta_\theta - \sin\theta\sin\delta_\theta + j\sin\theta\cos\delta_\theta + j\cos\theta\sin\delta_\theta + \cos(\theta+\phi)\cos(\delta_\theta+\delta_\phi) - \sin(\theta+\phi)\sin(\delta_\theta+\delta_\phi) + j\sin(\theta+\phi)\cos(\delta_\theta+\delta_\phi) + j\cos(\theta+\phi)\sin(\delta_\theta+\delta_\phi) - \cos\theta - j\sin\theta - \cos(\theta+\phi) - j\sin(\theta+\phi)$. Similar to the proof of Lemma 1, let us apply approximations for high quantization resolution, $\cos\delta_\theta \approx 1$, $\cos(\delta_\theta+\delta_\phi) \approx 1$, $\sin\delta_\theta \approx \delta_\theta$, and $\sin(\delta_\theta+\delta_\phi) \approx \delta_\theta + \delta_p$ and we get $\hat{c} - c \approx -\delta_\theta\sin\theta - (\delta_\theta+\delta_\phi)\sin(\theta+\phi) + j\delta_\theta\cos\theta + j(\delta_\theta+\delta_\phi)\cos(\theta+\phi)$. Combining the terms yields $|\hat{c}-c|^2 \approx 2\delta_\theta^2(1+\cos\phi) + \delta_\phi^2 + 2\delta_\theta\delta_\phi(1+\cos\phi)$. Note that $(1+\cos\phi) = 2\cos^2(\phi/2)$, which is equal to $r^2/2$ as $\phi = 2\cos^{-1}(r/2)$. It follow that $|\hat{c}-c|^2 \approx \delta_\theta^2 r^2 + \delta_\phi^2 + \delta_\theta\delta_\phi r^2$. As δ_θ and δ_ϕ have zero mean and they are uncorrelated, we arrive at (5).

Appendix C. Proof of (8)

The quantization error can be expressed as

$$\hat{c} - c = 2e^{j\alpha}(e^{j\delta_\theta}\cos((\phi+\delta_\phi)/2) - \cos(\phi/2))$$
$$\approx 2e^{j\alpha}(\delta_\phi/2\sin(\phi/2) + j\delta_\theta\cos(\phi/2)),$$

where we have applied the approximations for high resolution quantization, $\cos\delta_\theta \approx 1$, $\sin\delta_\theta \approx \delta_\theta$, $\cos(\delta_\phi/2) \approx 1$ and $\sin(\delta_\phi/2) \approx \delta_\phi/2$. The above equation leads to the MSE expression in (8).

7. REFERENCES

[1] Z. Pi and F. Khan, "An introduction to millimeter-wave mobile broadband systems," IEEE Communications Magazine, vol. 49, no. 6, pp. 101-107, June 2011.

[2] X. Zhang, A. F. Molisch and S. Y. Kung, "Variable-phase-shift-based RF-baseband codesign for MIMO antenna selection," IEEE Trans. Signal Processing, vol. 53, no. 11, pp. 4091-4103, Nov. 2005.

[3] O. E. Ayach, S. Rajagopal, S. Abu-Surra, Z. Pi, R. W. Heath Jr, "Spatially sparse precoding in millimeter wave MIMO systems," IEEE Transactions on Wireless Communications, vol. 99, pp. 1-15, Jan. 2014.

[4] E. Zhang and C. Huang, "On achieving optimal rate of digital precoder by RF-baseband codesign for MIMO systems," Proceedings of IEEE Vehicular Technology Conference, Sep. 2014

[5] J. A. Zhang, X. Huang, V. Dyadyuk, and Y. J. Guo, "Massive hybrid antenna array for millimeter-wave cellular communications," *IEEE Wireless Communications*, pp. 79-87, Feb. 2015.

[6] A. Alkhateeb, J. Mo, N. G. Prelcic, and R. W. Heath Jr, "MIMO precoding and combining solutions for millimeter-wave systems," IEEE Communications Magazine, vol.52, no.12, pp.122-131, Dec. 2014.

[7] A. Gersho and R. M. Gray, Vector Quantization and Signal Compression, Kluwer Academic Publishers, 1991.

[8] P. P. Vaidyanathan, *Multirate Systems and Filter Banks*, Prentice-Hall, 1993.

[9] K. I. Pedersen, P. E. Mogensen, and B. H. Fleury, "The Power Azimuth Spectrum in Outdoor Environments", IEE Electronics Letters, vol. 33, no. 18, pp. 1583-1584, Aug. 1997.

[10] V. Erceg, et al., "TGn channel models, IEEE 802.11-03/940r4, May 2004.

[11] Yuan-Pei Lin, "On the quantization of phase shifters for hybrid precoding systems," submitted to IEEE Trans. Signal Processing.